Almholt, K. et al. Metastasis of transgenic breast cancer in plasminogen activator inhibitor-1 gene-deficient mice. Oncogene 22, 4389-4397

ARTICLE *in* ONCOGENE · AUGUST 2003

Impact Factor: 8.46 · DOI: 10.1038/sj.onc.1206601 · Source: PubMed

6 AUTHORS, INCLUDING:

Kasper Almholt
Novo Nordisk
29 PUBLICATIONS **1,251** CITATIONS
SEE PROFILE

Boye Schnack Nielsen
Bioneer AS
103 PUBLICATIONS **4,187** CITATIONS
SEE PROFILE

Thomas L. Frandsen
University of Copenhagen, Rigshospitalet
38 PUBLICATIONS **1,222** CITATIONS
SEE PROFILE

Morten Johnsen
University of Copenhagen
29 PUBLICATIONS **1,882** CITATIONS
SEE PROFILE

Oncogene (2003) 22, 4389–4397

www.nature.com/onc

Metastasis of transgenic breast cancer in plasminogen activator inhibitor-1 gene-deficient mice

Kasper Almholt*,[1], Boye S Nielsen[1], Thomas L Frandsen[1], Nils Brünner[1,3], Keld Danø[1], Morten Johnsen[1,2]

[1]*The Finsen Laboratory, Rigshospitalet, Strandboulevarden 49, DK-2100 Copenhagen, Denmark;* [2]*Institute of Molecular Biology, University of Copenhagen, Øster Farimagsgade 2A, DK-1353 Copenhagen, Denmark*

The plasminogen activator inhibitor-1 (PAI-1) blocks the activation of plasmin(ogen), an extracellular protease vital to cancer invasion. PAI-1 is like the corresponding plasminogen activator uPA (urokinase-type plasminogen activator) consistently expressed in human breast cancer. Paradoxically, high levels of PAI-1 as well as uPA are equally associated with poor prognosis in cancer patients. PAI-1 is thought to play a vital role for the controlled extracellular proteolysis during tumor neovascularization. We have studied the effect of PAI-1 deficiency in a transgenic mouse model of metastasizing breast cancer. In these tumors, the expression pattern of uPA and PAI-1 resembles that of human ductal breast cancer and plasminogen is required for efficient metastasis. In a cohort of 63 transgenic mice that were either PAI-1-deficient or wild-type sibling controls, primary tumor growth and vascular density were unaffected by PAI-1 status. PAI-1 deficiency also did not significantly affect the lung metastatic burden. These results agree with the virtual lack of spontaneous phenotype in PAI-1-deficient mice and humans and may reflect that the plasminogen activation reaction is not rate limiting for tumor vascularization and metastasis, or that there is a functional redundancy between PAI-1 and other inhibitors of the uPA/plasmin system, masking the effect of PAI-1 deficiency.
Oncogene (2003) **22,** 4389–4397. doi:10.1038/sj.onc.1206601

Keywords: plasminogen activator inhibitor-1 (PAI-1); metastasis; breast cancer; angiogenesis

Introduction

Tissue remodeling during normal and pathological processes such as embryogenesis (Werb *et al*., 1999), mammary gland morphogenesis (Werb *et al*., 1996; Lund *et al*., 2000), wound healing (Lund *et al*., 1999), angiogenesis (Pepper, 2001) and cancer invasion (Johnsen *et al*., 1998; Matrisian, 1999; Stamenkovic, 2000) is finely regulated by the presence of extracellular matrix-degrading proteases and their corresponding inhibitors. Among the various extracellular proteolytic cascades, the plasminogen activation (PA) system has a well-documented role in most of these processes, including cancer invasion (Rømer *et al*., 1996; Bugge *et al*., 1998; Johnsen *et al*., 1998; Lund *et al*., 2000).

The PA system (Tapiovaara *et al*., 1996; Andreasen *et al*., 2000; Lijnen, 2001; Parfyonova *et al*., 2002) leads to generation of the broad-spectrum serine protease plasmin from its circulating zymogen. Plasminogen is proteolytically activated by specific activators. The urokinase-type plasminogen activator (uPA), the most cancer relevant plasminogen activator, is synthesized as the zymogen pro-uPA. Pro-uPA binds with high affinity to a cell surface-bound receptor, the urokinase receptor (uPAR). Receptor binding of pro-uPA concomitant with cell surface binding of plasminogen strongly enhances the overall reaction leading to plasmin formation and at the same time localizes plasmin activity to cell surfaces. The PA cascade is inhibited at several levels by serpin-type protease inhibitors. The main plasmin inhibitor is α_2-antiplasmin, while plasmin formation is inhibited by at least two plasminogen activator inhibitors, PAI-1 and PAI-2. Of these, PAI-1 is considered to be the primary physiological extracellular inhibitor of plasminogen activation. It rapidly inhibits both free and receptor-bound uPA as well as the tissue-type plasminogen activator (tPA), the main thrombolytic plasminogen activator. PAI-1 that is not complexed with a plasminogen activator has a high affinity for vitronectin, an interaction that may play a role in cellular adhesion and migration (Deng *et al*., 1996; Loskutoff *et al*., 1999).

uPA, uPAR and also PAI-1 are consistently expressed in invasive areas of human breast cancer (Pyke *et al*., 1993; Bianchi *et al*., 1995; Nielsen *et al*., 1996), and also in a wide variety of other human cancers, including carcinomas of the colon, lung, ovary and prostate (Hewitt and Danø, 1996; Andreasen *et al*., 1997). In addition to the epithelial component, carcinomas consist of a variety of stromal cells, such as fibroblasts, endothelial cells and macrophages. The components of the uPA system are often expressed by stromal cells rather than the epithelial cancer cells, in a pattern that is

*Correspondence: K Almholt, The Finsen Laboratory, Rigshospitalet dept. 8621, Strandboulevarden 49, DK-2100 Copenhagen, Denmark; E-mail: kasper@finsenlab.dk

[3]Present address: Institute of Pharmacology and Pathobiology, The Royal Veterinary and Agricultural University, Ridebanevej 9, DK-1870 Frederiksberg, Denmark

Received 26 August 2002; revised 5 March 2003; accepted 21 March 2003

characteristic for each type of cancer (Hewitt and Danø, 1996; Johnsen *et al*., 1998; Almholt and Johnsen, in press). In ductal mammary carcinoma, uPA is thus mainly expressed by myofibroblasts (Nielsen *et al*., 1996, 2001b), uPAR by macrophages (Pyke *et al*., 1993; Bianchi *et al*., 1994), while PAI-1 immunoreactivity is present in fibroblasts, endothelial cells, macrophages and some cancer cells (Bianchi *et al*., 1995).

In breast cancer and several other types of cancer, high levels of uPA and uPAR in the cancer tissue are strongly associated with poor prognosis, in agreement with the proposed enhancing role of both molecules in matrix degradation and cancer invasion (Duffy *et al*., 1988; Grøndahl-Hansen *et al*., 1993, 1995; Look *et al*., 2002; Riisbro *et al*., 2002). Surprisingly, high levels of the inhibitory molecule PAI-1 in breast cancer tissue are also strongly and consistently associated with poor prognosis, that is, short survival of the patients (Jänicke *et al*., 1991; Grøndahl-Hansen *et al*., 1993; Harbeck *et al*., 1999; Look *et al*., 2002), and a similar association has been found in several other types of cancer (Nekarda *et al*., 1994; Pedersen *et al*., 1994; Andreasen *et al*., 1997). The reason for this apparently paradoxical relation between PAI-1 and prognosis has not yet been clarified.

In spite of the thorough biochemical knowledge of PAI-1 and its interaction with uPA, tPA and vitronectin, little is known of the nonthrombolytic functions of this inhibitor *in vivo*. In patients with complete PAI-1 deficiency, the clinical manifestations appear to be restricted to abnormal bleeding after trauma (Fay *et al*., 1997). In PAI-1 gene-deficient mice there is only a mild acceleration of thrombolysis, but no apparent spontaneous extravascular abnormalities, a finding that may reflect that other protease inhibitors compensate for the lack of PAI-1 (Carmeliet *et al*., 1993a, b). However, it has been reported that host PAI-1 deficiency impairs tumor angiogenesis in both a transplanted murine skin cancer model (Bajou *et al*., 1998, 2001) and a transplanted murine fibrosarcoma (Gutierrez *et al*., 2000).

To obtain new information on the role of PAI-1 in breast cancer, we have now studied the effect of PAI-1 gene deficiency in transgenically induced breast cancer, thus avoiding the inherent problems of transplanting cancer cells, which themselves may produce PAI-1, into PAI-1-deficient mice. In this transgenic model, the polyomavirus middle T antigen (PymT) under control of a mouse mammary tumor virus long-terminal repeat promoter (MMTV-LTR) induces breast tumors with 100% penetrance (Guy *et al*., 1992). These are similar to human mammary adenocarcinoma, both with respect to histology and to expression of uPA and PAI-1 in stromal cells adjacent to invasive cancer cells. Furthermore, all the mice get lung metastases (Guy *et al*., 1992; Bugge *et al*., 1998), and we have previously found that the plasminogen activation system plays a role in metastasis, which is considerably delayed in plasminogen-deficient mice (Bugge *et al*., 1998). We here use a recently developed stereological method (Nielsen *et al*., 2001a) for a precise quantitation of the effect of PAI-1 deficiency on metastasis.

Materials and methods

Mice

Heterozygous FVB/N-TgN(*MMTVPyVT*)634 Mul (Guy *et al*., 1992) (hereafter FVB-*PymT*) male mice were mated with PAI-1 heterozygous females (Carmeliet *et al*., 1993a), which had been backcrossed for eight generations onto the C57BL/6J strain (B6-*Pai-1*$^{+/-}$(N8)). Their male F1 offspring were mated with the B6-*Pai-1*$^{+/-}$(N8) females to generate the B6,FVB-*PymT,Pai-1*$^{-/-}$, -*PymT,Pai-1*$^{+/+}$, -*Pai-1*$^{-/-}$ and -*Pai-1*$^{+/+}$ mice used throughout the study, all of which were siblings. All pups were weaned at age 21–23 days, genotyped and recaged randomly with six mice in each cage. Tissue for *in situ* hybridization studies was obtained from FVB-*PymT* and non-transgenic FVB females unless otherwise stated. All analyzed mice were female virgins. All animal experiments were approved by the Danish Animal Experiments Inspectorate. The mice were housed in a restricted access facility and fed a regular chow. A concurrent FELASA compliant health report revealed no infections.

Genotyping

Chromosomal DNA from an approx. 2-mm piece of tail tip was isolated essentially as described (Laird *et al*., 1991). Genotyping was performed by combining in a single PCR reaction a primer pair specific for the MMTV-PymT transgene (Bugge *et al*., 1998) with three primers specific for the PAI-1 alleles. mPAI1.1p (TTC ATG CCC TCT GGT CGC TG) upstream and mPAI1.2 m (CTC CCT CCC TCC CAG TGA CTT G) downstream of the 5′ insertion point of the targeting vector (i.e. the *Xho*I(911) site in the PAI-1 gene promoter region, GenBank: M33961) amplified a 349 bp band specific for the endogenous allele. The 5′ end of the inserted DNA fragment in the disrupted PAI-1 allele (Carmeliet *et al*., 1993a) is a *Xho*I-*Bam*HI neomycin cassette from pPNT (Tybulewicz *et al*., 1991). mPAI1.1p and mPGK2 m (GCC TTG GGA AAA GCG CCT C) in the mouse phosphoglycerate kinase-1 promoter (GenBank: M18735) within this neomycin cassette amplified an approx. 220 bp band specific for the disrupted allele. In all, 35 cycles of PCR with T(anneal) = 60°C were performed using HotStarTaq (Qiagen, Cat# 203445, Hilden, Germany) as described by the manufacturer.

Tumor growth and tissue processing

Mice were examined weekly for mammary tumor onset by palpation for nodules in all 10 mammary glands by a person unaware of their genotype. The date of first positive diagnosis was taken as the date the first tumor was found, provided that the diagnosis was confirmed the following week. Tumor volume was assessed weekly by measuring the length and width of individual tumors with a caliper. The volume of each tumor was approximated as the volume of an oblong spheroid of the measured length (l) and width (w) that is $V(\text{tumor}) = \pi l w^2/6$ (Euhus *et al*., 1986). The individual tumor volumes were summed to give the total tumor volume in each mouse. To minimize final tumor size variation, the mice were killed 5–6 days after the total tumor burden in each individual mouse exceeded a preset threshold size of 1.5 cm^3. The mice were anesthetized as described (Lund *et al*., 2000) and a tumor sample was collected for RNA analysis and immediately

placed on dry ice. Hereafter, the mice were perfusion fixed with 10 ml cold Dulbecco's phosphate-buffered saline (PBS) (Biochrom, Cat# L1825, Berlin, Germany) followed by 10 ml freshly prepared cold PBS with 4% paraformaldehyde (Merck, Darmstadt, Germany). Their lungs were removed, air-evacuated, fixed and cryoembedded for metastasis quantification as described (Nielsen *et al*., 2001a). Tumor tissue for *in situ* hybridization and CD34 staining was removed, cut into ~5-mm thick slabs for optimal access of fixative and placed in PBS with 4% paraformaldehyde overnight at 4°C before automated paraffin embedding (Thermo Shandon, Cat# 75200011, Pittsburgh, PA, USA). Two slabs of the largest tumor from each mouse were prepared for CD34 staining.

Northern blotting

Frozen tumor tissue was ground with a mortar and pestle and disrupted with a mechanical tissue homogenizer. Total RNA was extracted using the RNeasy kit (Qiagen, Cat# 75142) as described by the manufacturer. A measure of 10 μg of each sample was denatured and electrophoresed by the glyoxal/DMSO method (Brown and Mackey, 1997) and transferred to a nylon membrane (Bio-Rad, Cat# 162-0196, Hercules, CA, USA) by upward capillary transfer in 10 mM NaOH for 2 h. The RNA was UV-crosslinked to the membrane and incubated overnight at 68°C with a [^{32}P]UTP-labeled RNA probe at 10^6 c.p.m./ml in 50% formamide, 0.12 M NaH_2PO_4 pH 7.0, 0.25 M NaCl, 7% SDS, and 0.1 mg/ml yeast tRNA (GibcoBRL, Cat# 15401-029). The membrane was washed the following day at 65°C with 0.1% SDS in saline citrate buffers (SSC) of decreasing strength, and exposed on a phophorimager screen.

Radiolabeled RNA probes were transcribed from plasmids containing fragments of various mouse cDNAs and hybridized separately to identical membranes. The plasmids were pmuPA10 K that contains a 201–608 *Eco*RI fragment of uPA (GenBank: X02389) in pBluescript KS+; the plasmid pKaA229 that contains an *Eco*RI(804)-2497 fragment of tPA (GenBank: J03520) in pT7T3-18; the Image Consortium Clone ID 1226790 (Lennon *et al*., 1996) that contains a fragment of PAI-2; the plasmid pmPAI-1 03 K that contains a *Pst*I(338)-*Xho*I(857) fragment of PAI-1 (GenBank: M33960) in pBluescript KS+; and the plasmid pKaA127 that contains a 51–1033 fragment of glyceraldehyde-3-phosphate dehydrogenase (GAPDH; GenBank: M32599) in pCR2.1. The plasmid pmuPA10 K was subcloned from pmuPA10 (Kristensen *et al*., 1991), while pKaA229 was subcloned from pTAM50, which was kindly provided by Dr RJ Rickles. Each plasmid was linearized in order to transcribe fragments of 408-821 bp.

In situ *hybridization*

PAI-1 mRNA was detected in tissue samples using [^{35}S]UTP-labeled RNA probes at 10^5 c.p.m./µl on 5-μm thick paraffin sections essentially as described (Kristensen *et al*., 1991). The sections were developed after 2 weeks of exposure and counterstained lightly with hematoxylin and eosin (H&E). The RNA probes were transcribed in antisense or sense orientation from two nonoverlapping fragments of mouse PAI-1 cDNA (Prendergast *et al*., 1990) in pBluescript KS+: plasmids pmPAI-1 02 (8–338 PstI fragment) and pmPAI-1 03 K.

Vascular length density quantification

Paraffin sections (5-μm) were dried overnight at room temperature, deparaffinized in xylene and hydrated through graded ethanol solutions. The sections were boiled twice for 5 min in 10 mM citric acid pH 6.0 in a microwave oven to demask the antigen, then slowly cooled to room temperature, where all the following steps were performed. Endogenous peroxidases were exhausted by 15 min incubation in fresh 1% H_2O_2. The sections were rinsed in tap water, transferred to Tris-buffered saline (50 mM Tris pH 7.6, 150 mM NaCl) with 0.5% Triton X-100 and mounted in disposable immunostaining chambers (Thermo Shandon, Cat# 7211013). Prior to incubation, the previously characterized monoclonal rat anti-mouse CD34 antibody (Garlanda *et al*., 1997) (HyCult Biotechnology, Cat# HM1015, Uden, The Netherlands) was biotinylated (non-chemically) using the DAKO ARK kit (DAKOCytomation, Cat# K3955, Glostrup, Denmark) as described by the manufacturer. Although intended for mouse antibodies, the ARK kit crossreacts with rat antibodies as stated by the manufacturer. The sections were incubated with the biotinylated anti-CD34 antibody (final conc. 3.3 μg/ml) for 2 h. Addition of streptavidin-conjugated peroxidase and color development with 3,3-diaminobenzidine · 4HCl (DAB) was performed as described in the ARK kit. The sections were lightly counterstained with hematoxylin, rinsed in tap water, removed from the staining chambers and mounted with glycergel (DAKOCytomation, Cat# C563). A mouse monoclonal antitrinitrophenyl antibody (Shulman *et al*., 1978) was biotinylated and used in parallel as a negative control.

Vascular length density L_V(vasc/tumor) (1) was estimated with an unbiased stereological technique (Frandsen *et al*., 2001) on two CD34-stained tumor sections from each mouse. Vascular profiles Q(vasc) were identified by two criteria: positive staining for CD34 and morphological resemblance of a vessel. P(tumor) is a point count used to estimate the analyzed tumor tissue area; $a(p)$ is the area associated with each point.

$$L_V(\text{vasc/tumor}) = 2\sum Q(\text{vasc}) \Big/ \Big(a(p)\sum P(\text{tumor})\Big) \quad (1)$$

The average radius of living tumor around a vessel $\bar{r}$(tumor/vasc) (2) (including the vessel radius) was also calculated.

$$\bar{r}(\text{tumor/vasc}) = [\pi L_V(\text{vasc/tumor})]^{-0.5} \quad (2)$$

Stereological quantification of lung metastasis volume

Gundersen *et al*. described the general principles behind stereological volume estimations (Gundersen *et al*., 1988). The estimate of total metastasis volume in each set of lungs was obtained using a recently developed unbiased and precise computer-assisted stereological technique (Nielsen *et al*., 2001a). Briefly, the cryoembedded lungs were cut into slabs of 2-mm thickness (t) to obtain 5–8 evenly distributed cross-sections, which were then reembedded face down in a single block, sectioned and H&E stained. All observations were done by a person unaware of the genotype of the analyzed specimens.

The total metastasis volume V(met) (3) was calculated from a point count P(met) used to estimate the area of metastatic foci in the sections. $a(p)$ is the area associated with each point.

$$V(\text{met}) = ta(p)\sum P(\text{met}) \quad (3)$$

Statistical analyses

Hypotheses on differences between genotypes with respect to tumor latency, age at sacrifice, final tumor volume and vascular length density were tested by Student's *t*-tests. The rate of tumor growth for each mouse was estimated by linear regression of all (logarithmically transformed) tumor measurements from the first time the mouse presented with a palpable tumor and until it was killed. The tumor growth rates were then analyzed by Student's *t*-test. Metastasis incidence was analyzed by Fisher's exact test. Metastasis volumes were transformed logarithmically and analyzed by Student's *t*-test. To allow logarithmic transformation, tumor and metastasis volumes of zero were given values of 10^{-4} cm^3 and 10^{-4} mm^3, respectively. In all analyses, a P-value < 0.05 was considered significant. Values are given as average $\pm$ s.d. if not otherwise stated. The SAS® software package (ver. 8.0; SAS Institute, Cary, NC, USA) was used to perform the statistical analyses.

Results

Histology and PAI-1 expression in MMTV-PymT-induced tumors

Tissue was obtained from 13–15 week old FVB-*PymT* females unless otherwise stated. The MMTV-PymT tumors resembled human mammary adenocarcinomas as previously described (Guy *et al*., 1992; Bugge *et al*., 1998; Maglione *et al*., 2001). There were no obvious morphological differences in the analyzed late stage tumors as a consequence of PAI-1 deficiency. We used *in situ* hybridization to analyze the expression pattern of PAI-1 mRNA in MMTV-PymT-induced mammary tumors and lung metastases. In 10 of 10 cases, we detected PAI-1 mRNA in stromal cells within and surrounding the primary tumors, usually concentrated at the periphery (including invasive fronts) (Figure 1a–d). In no cases could we detect PAI-1 mRNA in the neoplastic epithelial cells. Similarly, in six of nine cases analyzed, we detected PAI-1 mRNA in stromal cells within and surrounding metastatic foci in the lungs (Figure 1e–h). Again, in no case could we detect PAI-1 mRNA in the epithelial cells of the metastases. In three sets of lungs, two of which also contained PAI-1 mRNA positive metastases, we additionally found PAI-1 mRNA in a number of scattered cells that were not associated with metastatic foci (data not shown). We detected very little or no PAI-1 expression in lungs from age- and background-matched nontransgenic FVB mice ($n = 3$; data not shown). We confirmed the hybridization specificity with three different approaches: we did not observe any PAI-1 mRNA signal in primary tumors from B6,FVB-*PymT,Pai-1*$^{-/-}$ mice ($n = 2$; data not shown), and on adjacent sections of every tissue analyzed, we obtained similar results with a nonoverlapping antisense RNA probe (data not shown) and saw no signal with the corresponding sense probes (Figure 1c and g). To exclude strain-specific differences, we confirmed that tumors from B6,FVB-*PymT,Pai-1*$^{+/+}$ mice stained positive for PAI-1 mRNA (data not shown).

Tumor growth and vascularity in PAI-1 gene-deficient mice

In order to determine the influence of PAI-1 deficiency on MMTV-PymT-induced tumors, we generated a cohort consisting of *PymT,Pai-1*$^{-/-}$ ($n = 24$), *PymT,Pai-1*$^{+/+}$ ($n = 39$) and non-transgenic *Pai-1*$^{-/-}$ ($n = 11$) and *Pai-1*$^{+/+}$ ($n = 9$) mice – all siblings. No unscheduled deaths took place in the cohort. An observer unaware of individual genotypes measured the tumor burden of

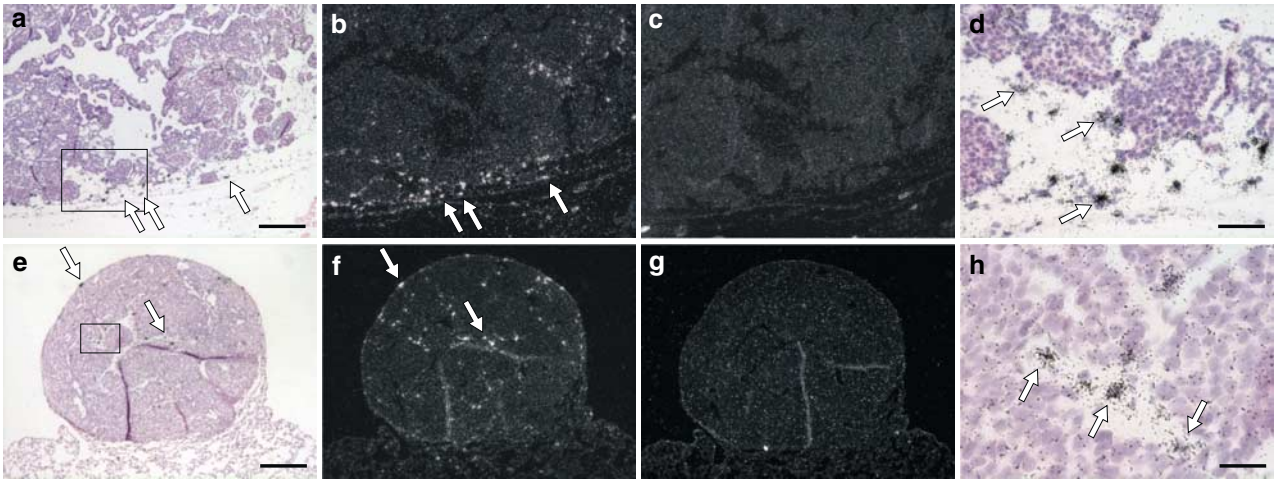

Figure 1 Expression of PAI-1 mRNA in MMTV-PymT-induced mammary tumors and lung metastases. PAI-1 mRNA was detected by *in situ* hybridization in primary tumors (**a**–**b**) and lung metastases (**e**–**f**) with a PAI-1 antisense RNA probe. Staining is seen as silver grains in the bright field images (**a**, **e**) and more readily with dark field illumination as white reflections (**b**, **f**). Hybridizations with the corresponding sense RNA probe were negative (**c**, **g**). PAI-1 mRNA was abundant at the invasive front of the primary MMTV-PymT-induced breast tumors (corresponding arrows in **a**, **b**). PAI-1 mRNA was also seen in scattered cells in some lung metastases, here shown in a large surface metastasis (corresponding arrows in **e**, **f**). Higher magnifications of the areas indicated in **a** and **e** illustrate that PAI-1 mRNA was primarily found in stromal cells in the connective tissue of both the primary tumors (**d**) and lung metastases (**h**). Sections were H&E counterstained. Bars are 200 μm (**a**, **e**), 50 μm (**d**), and 25 μm (**h**)

each mouse weekly. All the MMTV-PymT-transgenic mice developed tumors irrespective of their PAI-1 status. The primary tumors of PAI-1-deficient and control mice first appeared at ages 61 ± 13 and 63 ± 11 days, respectively. Thus, there was no significant difference in the age at tumor detection (*t*-test, $P = 0.43$; Figure 2).

As detailed in the 'Materials and Methods' section, the mice were killed as soon as their total tumor volume had passed a threshold level of 1.5 cm^3. This was done to ensure that a possible effect on tumor vascularity and metastatic burden was not simply a reflection of different primary tumor size in the animals. The PAI-1-deficient and control mice passed the preset threshold at average ages of 122 ± 15 and 126 ± 12 days, respectively; this difference was not significant (*t*-test, $P = 0.22$; Figure 2). As a result of this strategy, the primary tumor volumes at the day of sacrifice were very similar: 2.62 ± 0.6 cm^3 in PAI-1-deficient vs 2.55 ± 0.9 cm^3 in control mice (*t*-test, $P = 0.72$).

The total tumor volume of each mouse was measured weekly and transformed logarithmically before calculating their average $\pm$ s.d. (Figure 3). The exponential tumor growth rate of each mouse was estimated by linear regression of all (logarithmically transformed) tumor measurements from the first time the mouse presented with a palpable tumor and until it was killed. The exponential tumor growth rates of *PymT,Pai-1*$^{-/-}$ mice were on average slightly higher than those of *PymT,Pai-1*$^{+/+}$ mice, but they did not differ significantly (*t*-test, $P = 0.11$). The average tumor volume doubling times were 6.8 ± 1.7 days in PAI-1-deficient vs 7.2 ± 1.4 days in control mice.

As earlier reports have shown an effect of PAI-1 deficiency on vascularization in some transplanted tumor model systems (Bajou *et al*., 1998, 2001; Gutierrez *et al*., 2000), we also analyzed the tumor vascularity. A palpable tumor does not usually develop in all 10 mammary glands. Therefore, it would not be possible to analyze a tumor from the same gland in all mice. Instead, we used the largest tumor from each mouse. The tumor vascular density was quantified on two CD34-stained sections from each tumor (Figure 4). All of the analyzed tumors were judged to be adequately and evenly fixed, as none of them displayed a conspicuous absence of CD34 staining. The vascular length density (mm vessel/mm^3) in the analyzed primary tumors was slightly, but not significantly, decreased in PAI-1-deficient mice to 68 ± 19 mm^{-2} vs 77 ± 23 mm^{-2} in control mice (*t*-test, $P = 0.13$; Figure 4). From this we calculated the average radius of living tumor around each vessel (including the vessel radius) to be 70 ± 10 μm in PAI-1-deficient vs 66 ± 9 μm in control mice.

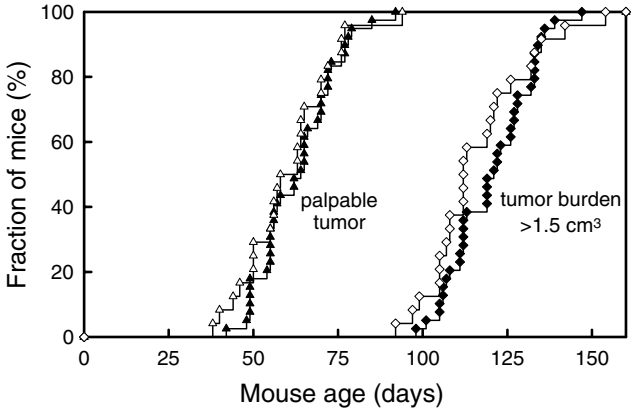

Figure 2 Primary tumor development in *PymT,Pai-1*$^{-/-}$ and *PymT,Pai-1*$^{+/+}$ mice. Tumor development and size were monitored weekly in a cohort of 24 *PymT,Pai-1*$^{-/-}$ mice and 39 *PymT,Pai-1*$^{+/+}$ sibling controls. When their total primary tumor burden had exceeded a threshold volume of 1.5 cm^3, the mice were killed and tumor tissue and lungs were removed for analysis. Fraction of tumor-bearing mice of the *PymT,Pai-1*$^{+/+}$ (▲) and *PymT,Pai-1*$^{-/-}$ (△) genotypes as a function of age, and fraction of *PymT,Pai-1*$^{+/+}$ (◆) and *PymT,Pai-1*$^{-/-}$ (◇) mice whose primary tumor burden had exceeded the threshold volume as a function of age

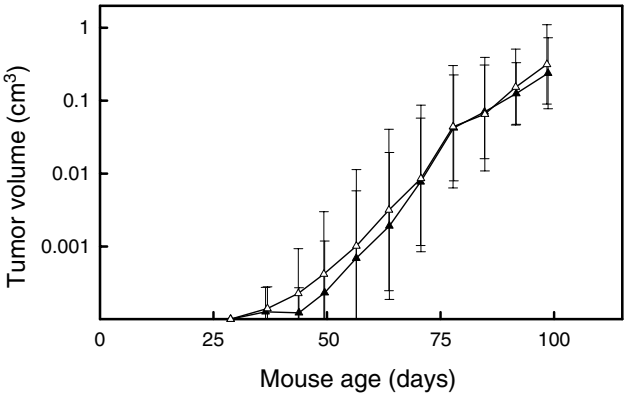

Figure 3 Primary tumor growth in *PymT,Pai-1*$^{-/-}$ and *PymT, Pai-1*$^{+/+}$ mice. Tumor size was monitored weekly in a cohort of 24 *PymT,Pai-1*$^{-/-}$ mice and 39 *PymT,Pai-1*$^{+/+}$ sibling controls. The geometric average of tumor volumes plotted vs age of the *PymT,Pai-1*$^{+/+}$ (▲) and *PymT,Pai-1*$^{-/-}$ (△) mice. These curves are not plotted past age 98 days since the first mouse was killed at this age after its tumor burden reached the threshold volume. Error bars: s.d. of logarithmically transformed data

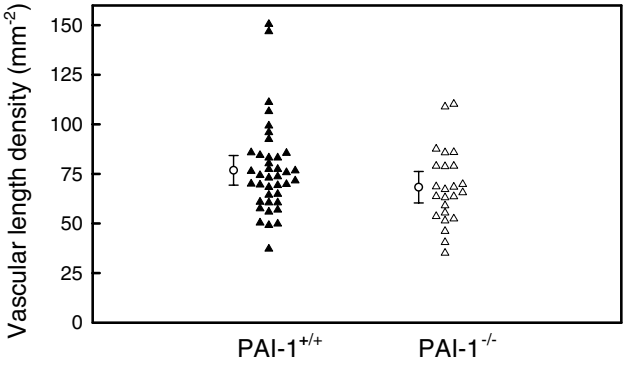

Figure 4 Tumor vascular length density in *PymT,Pai-1*$^{-/-}$ and *PymT,Pai-1*$^{+/+}$ mice. In total, 24 *PymT,Pai-1*$^{-/-}$ mice and 39 *PymT,Pai-1*$^{+/+}$ siblings were killed as described in the legend to Figure 2. Vascular length density (mm vessel/mm^3) was quantified from two CD34-stained sections of the largest tumor from each of the *PymT,Pai-1*$^{+/+}$ (▲) and *PymT,Pai-1*$^{-/-}$ Larger (△) mice. Average vascular length densities and their 95% confidence intervals are indicated

Lung metastasis in PAI-1 gene-deficient mice

The similar primary tumor burdens allowed unbiased comparison of lung metastases. Lungs with visible surface metastases at necropsy were rare in the cohort, regardless of PAI-1 status. The total volume of lung metastases in each mouse was quantified by stereological analysis of 5–8 evenly spaced H&E-stained cross-sections of its lungs (Nielsen *et al*., 2001a). Using this technique, we found 100% (24/24) incidence of lung metastases in PAI-1-deficient mice vs 92% (36/39) in control mice. This difference was not significant (Fisher exact, $P=0.28$). Lungs from the nontransgenic but sibling *Pai-1*$^{+/+}$ ($n=9$) and *Pai-1*$^{-/-}$ ($n=11$) mice were processed in parallel and included randomly among the analyzed lungs; none were scored positive for metastases.

The geometric average metastasis volume was increased to 0.165 mm^3 in PAI-1-deficient mice compared with 0.059 mm^3 in control mice (Figure 5). This seemingly large difference is not significant (*t*-test, $P=0.23$), reflecting inherent wide variation in metastatic burdens in mice of the same genotype.

Expression of PAI-2, uPA and tPA in PAI-1-deficient and wild-type tumors

To address the possibility that other components of the plasminogen activation system may be up- or down-regulated as a consequence of PAI-1 deficiency, we performed a Northern blot analysis of the expression level of PAI-2, uPA and tPA mRNAs in primary breast tumors from five *PymT,Pai-1*$^{-/-}$ and five *PymT,Pai-1*$^{+/+}$ mice (Figure 6). PAI-1-deficient and -proficient tumor samples for RNA extraction were processed in parallel and chosen in such a way that they pairwise came from mice killed on the same day. There were no apparent differences in the expression level of PAI-2, uPA, or tPA that could be related to PAI-1 status. The RNA samples were also hybridized with a PAI-1 probe confirming that PAI-1 mRNA was easily detected in *PymT,Pai-1*$^{+/+}$ tumors and undetectable in *PymT,Pai-1*$^{-/-}$ tumors (Figure 6).

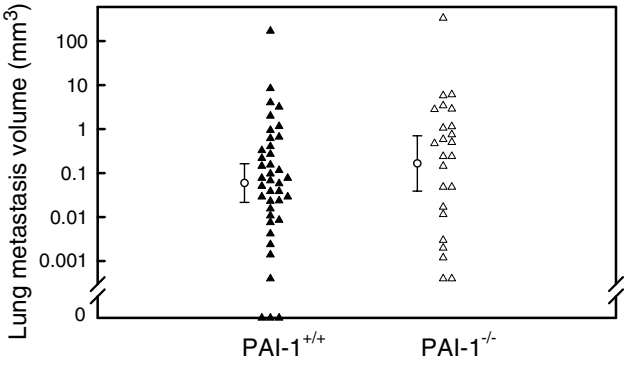

Figure 5 Lung metastasis volumes in *PymT,Pai-1*$^{-/-}$ and *PymT,Pai-1*$^{+/+}$ mice. In all, 24 *PymT,Pai-1*$^{-/-}$ mice and 39 *PymT,Pai-1*$^{+/+}$ siblings were killed as described in the legend to Figure 2. Total metastasis volume was quantified with an unbiased stereological technique (Nielsen *et al*., 2001a) on 5–8 evenly spaced H&E-stained sections of the lungs from each of the *PymT,Pai-1*$^{+/+}$ (▲) and *PymT,Pai-1*$^{-/-}$ (△) mice. Geometric average metastasis volumes and their 95% confidence intervals are indicated

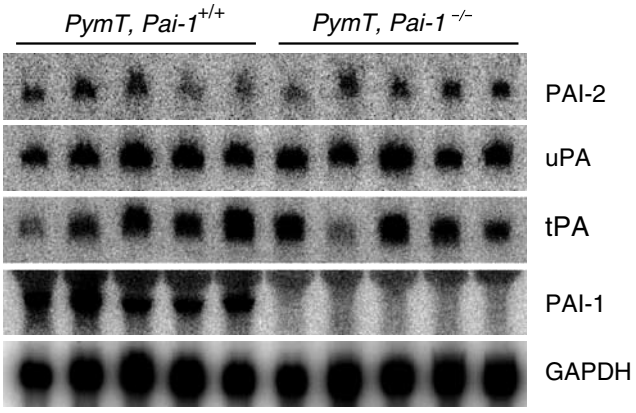

Figure 6 PAI-2, uPA, and tPA mRNAs in *PymT,Pai-1*$^{-/-}$ and *PymT,Pai-1*$^{+/+}$ mammary tumors. Total RNA from five *PymT,Pai-1*$^{-/-}$ and 5 *PymT,Pai-1*$^{+/+}$ primary tumors were analyzed by Northern blotting for expression of PAI-2, uPA and tPA mRNAs. Expressions of PAI-1 and GAPDH mRNAs were included as controls

Discussion

We have analyzed the consequences of PAI-1 deficiency on tumor development, growth, vascularity and metastasis in a transgenic mouse model. In this model, the MMTV-PymT transgene results in the development of mammary tumors in all virgin females and virtually all tumors eventually metastasize to the lungs (Guy *et al*., 1992; Bugge *et al*., 1998). Both uPA (Bugge *et al*., 1998) and PAI-1 are present in stromal cells in these tumors, as they are in human ductal adenocarcinomas of the breast (Wolf *et al*., 1993; Bianchi *et al*., 1995; Nielsen *et al*., 1996, 2001b), and inactivation of the plasminogen gene leads to reduced lung metastasis, thus demonstrating a role of the PA system in this process (Bugge *et al*., 1998).

By crossing a PAI-1-null allele (Carmeliet *et al*., 1993a) into the MMTV-PymT model, we generated a cohort of mice in which we could compare tumor incidence, latency and growth rates while the animals were still alive. Tumor vascularity and lung metastasis burden were determined after killing of the mice, when their primary tumor volume had reached a previously set threshold value. Thus, these parameters would not be influenced by variations in the size of the primary tumors. Analysis of a total of 24 *PymT,Pai-1*$^{-/-}$ mice and 39 *PymT,Pai-1*$^{+/+}$ siblings showed no significant differences between PAI-1-deficient and wild-type animals in any of the analyzed parameters. We also found no evidence that PAI-1 deficiency lead to a compensatory increase in the alternative inhibitor PAI-2 or a

decrease in either of the plasminogen activators uPA and tPA. Such expression differences could potentially account for the lack of phenotype in the PAI-1-deficient mice. We therefore conclude that PAI-1 deficiency by itself does not significantly influence tumorigenesis, tumor growth, vascularization or metastasis in the MMTV-PymT model.

These findings agree well with the virtual lack of detectable spontaneous phenotype in PAI-1 gene-deficient mice (Carmeliet *et al*., 1993a, b), which indicates that development, growth and reproduction take place normally in the absence of PAI-1. Also in man, PAI-1 deficiency is without clinical manifestations, except for mild bleeding disorders (Fay *et al*., 1997). Nevertheless, plasminogen activation is thought to play a role in processes like implantation (Sappino *et al*., 1989; Hofmann *et al*., 1994; Feng *et al*., 2001), embryogenesis (Sappino *et al*., 1991; Häckel *et al*., 1995) and angiogenesis (Pepper, 2001), and PAI-1 is expressed during these processes (Hofmann *et al*., 1994; Häckel *et al*., 1995; Pepper *et al*., 1996; Feng *et al*., 2001).

Initially one might expect that PAI-1 deficiency increases plasminogen activation and thereby stimulates processes in which plasminogen activation is involved, such as metastasis in the MMTV-PymT model. However, it should be noted that the plasminogen activation reaction is only one step in a complex cascade of reactions that involve several additional steps, such as receptor binding of pro-uPA, cell surface binding of plasminogen and pro-uPA activation. Furthermore, the PA system is only one of several extracellular protease systems involved in invasion and metastasis, and extracellular proteolysis is only one of many factors involved in the overall process of metastasis. A possible explanation for the lack of effect of PAI-1 deficiency on metastasis of MMTV-PymT-induced tumors that we found in this study is, therefore, that the plasminogen activation reaction is not rate limiting for the overall process of metastasis in this model. Similar considerations apply to tumor vascularization. Additionally, there may be a functional overlap between PAI-1 and other protease inhibitors, either directly at the plasminogen activation step, or indirectly at other steps of the cascade. First of all, uPA-catalyzed plasminogen activation may also be inhibited by PAI-2, which primarily is found intracellularly but also appears to have extracellular functions (Montemurro *et al*., 1999); by the protein C inhibitor (España *et al*., 1993) and protease nexin-1 (Scott *et al*., 1985), both of which inhibit plasminogen activators among other serine proteases; and by maspin, which is a slow plasminogen activator inhibitor, but nevertheless may play an important physiological role because it promotes internalization of uPA and uPAR (Biliran and Sheng, 2001). The maspin gene also blocks tumor progression in a transplantation system based on the MMTV-PymT mouse (Shi *et al*., 2002). Secondly, it is highly likely that there is an indirect functional overlap between PAI-1 and inhibitors of plasmin activity, the main plasmin inhibitor being α_2-antiplasmin (Lijnen, 2001). Finally, inhibitors of pro-uPA activation may also substitute for the action of PAI-1; a candidate is hepatocyte growth factor activator inhibitor-1 (HAI-1), which inhibits the membrane-type serine protease matriptase (Lin *et al*., 1999), a pro-uPA activator (Takeuchi *et al*., 2000). We propose that a functional overlap of PAI-1 with another inhibitor requires that the second inhibitor is present in the tissue, but it need not be upregulated in the absence of PAI-1. We have shown that at least PAI-2 is expressed in the MMTV-PymT-induced primary tumors irrespective of PAI-1 status. Functional overlap between different molecules appears to be a widespread phenomenon and a reason for the lack of spontaneous phenotype often seen in mice made deficient in a single gene. For proteases specifically, we have previously shown that such an overlap exists between the PA system and matrix metalloproteases in wound healing (Lund *et al*., 1999). It remains to be investigated whether there is a similar functional overlap between PAI-1 and other protease inhibitors in metastasis of MMTV-PymT-induced tumors, for example, by the use of appropriate double knockout mice or by treatment of the PAI-1 gene-deficient mice with compounds that neutralize potentially overlapping protease inhibitors.

Previous studies have shown that host PAI-1 deficiency leads to reduced angiogenesis in a transplanted murine epithelial tumor model (Bajou *et al*., 1998, 2001) and a transplanted murine fibrosarcoma (Gutierrez *et al*., 2000), and it was recently reported that angiogenesis in a Matrigel implant assay (McMahon *et al*., 2001), an aortic explant assay (Devy *et al*., 2002), as well as a retinal model system (Lambert *et al*., 2001) is reduced or absent in PAI-1-deficient mice. There is an apparent discrepancy between the effect of PAI-1 deficiency in those studies and the lack of effect on tumor vascularization in MMTV-PymT-induced breast cancer that we report here, as well as the normal growth and development and the absence of spontaneous macroscopic and microscopic abnormalities in the PAI-1-deficient mice (Carmeliet *et al*., 1993a, b). A possible explanation for this discrepancy is that vascularization during development and during growth of endogenous tumors is governed by other processes than those that are provoked during transplanted tumor growth and in some experimental vascularization setups.

We have previously hypothesized that PAI-1 does not inhibit, but on the contrary promotes tumor progression by preventing excessive proteolysis (Andreasen *et al*., 1986; Kristensen *et al*., 1990; Danø *et al*., 1993; Grøndahl-Hansen *et al*., 1993). The assumption that PAI-1 promotes tumor progression has since been strongly supported by the consistent finding that *high* PAI-1 levels in tumor tissue are associated with *poor* prognosis in several types of human cancer (Jänicke *et al*., 1991; Nekarda *et al*., 1994; Pedersen *et al*., 1994; Andreasen *et al*., 1997). In human cancer tissue, PAI-1 is often expressed in endothelial cells (Pyke *et al*., 1991; Bianchi *et al*., 1995; Hewitt and Danø, 1996), and as an additional mechanism for a promoting role of PAI-1 in cancer progression,

it has been proposed that PAI-1 facilitates tumor angiogenesis (Pepper *et al*., 1996; Pepper, 2001). If PAI-1 plays a promoting role in tumor progression, it might be expected that PAI-1 deficiency would result in decreased tumor growth or metastasis. Our results clearly show that this is not the case in MMTV-PymT-induced breast cancer. This may reflect that PAI-1 does not play such a role in this model, but alternatively it may indicate functional overlap between PAI-1 and other protease inhibitors as discussed above.

Abbreviations

GAPDH, glyceraldehyde-3-phosphate dehydrogenase; H&E, hematoxylin and eosin; MMTV, mouse mammary tumor virus; PA, plasminogen activation; PAI, plasminogen activator inhibitor; PBS, phosphate-buffered saline; PymT, polyomavirus middle T antigen; tPA, tissue-type plasminogen activator; uPA, urokinase-type plasminogen activator; uPAR, urokinase-type plasminogen activator receptor.

Acknowledgements

We are indebted to Drs William J Muller and Peter Carmeliet for generously providing us with the MMTV-PymT and the PAI-1-deficient mice, respectively. We thank Agnieszka Ingvorsen, Pia Pedersen, Dorthe S. Olsen, Maria K. Kiersgaard and Mette M Lungholt for expert technical assistance, John Post for the photographic reproductions and Ib J Christensen for assistance with the statistical analyses. This work was supported by grants from Søren and Helene Hempels Foundation, Krista and Viggo Petersens Foundation, the Danish Research Agency and the Copenhagen Hospital Corporation.

References

Almholt K and Johnsen M. (in press). *Recent Results Cancer Res.,* **162**.

Andreasen PA, Egelund R and Petersen HH. (2000). *Cell Mol. Life Sci.,* **57,** 25–40.

Andreasen PA, Kjøller L, Christensen L and Duffy MJ. (1997). *Int. J. Cancer,* **72,** 1–22.

Andreasen PA, Nielsen LS, Kristensen P, Grøndahl-Hansen J, Skriver L and Danø K. (1986). *J. Biol. Chem.,* **261,** 7644–7651.

Bajou K, Masson V, Gerard RD, Schmitt PM, Albert V, Praus M, Lund LR, Frandsen TL, Brünner N, Danø K, Fusenig NE, Weidle U, Carmeliet G, Loskutoff D, Collen D, Carmeliet P, Foidart JM and Noël A. (2001). *J. Cell Biol.,* **152,** 777–784.

Bajou K, Noël A, Gerard RD, Masson V, Brünner N, Holst-Hansen C, Skobe M, Fusenig NE, Carmeliet P, Collen D and Foidart JM. (1998). *Nat. Med.,* **4,** 923–928.

Bianchi E, Cohen RL, Dai A, Thor AT, Shuman MA and Smith HS. (1995). *Int. J. Cancer,* **60,** 597–603.

Bianchi E, Cohen RL, Thor AT, Todd RF, Mizukami IF, Lawrence DA, Ljung BM, Shuman MA and Smith HS. (1994). *Cancer Res.,* **54,** 861–866.

Biliran Jr H and Sheng S. (2001). *Cancer Res.,* **61,** 8676–8682.

Brown T and Mackey K. (1997). *Current Protocols in Molecular Biology,* Vol. 1. Ausubel FM, Brent R, Kingston RE, Moore DD, Seidman JG, Smith JA, Struhl K (eds). John Wiley & Sons, Inc.: New York, pp 4.9.1–4.9.16.

Bugge TH, Lund LR, Kombrinck KK, Nielsen BS, Holmbäck K, Drew AF, Flick MJ, Witte DP, Danø K and Degen JL. (1998). *Oncogene,* **16,** 3097–3104.

Carmeliet P, Kieckens L, Schoonjans L, Ream B, van Nuffelen A, Prendergast G, Cole M, Bronson R, Collen D and Mulligan RC. (1993a). *J. Clin. Invest.,* **92,** 2746–2755.

Carmeliet P, Stassen JM, Schoonjans L, Ream B, van den Oord JJ, De Mol M, Mulligan RC and Collen D. (1993b). *J. Clin. Invest.,* **92,** 2756–2760.

Danø K, Grøndahl-Hansen J, Eriksen J, Nielsen BS, Rømer J and Pyke C. (1993). *Proteolysis and Protein Turnover,* Bond JS and Barrett AJ (eds) Portland Press Proceedings, pp 239–245.

Deng G, Curriden SA, Wang S, Rosenberg S and Loskutoff DJ. (1996). *J. Cell Biol.,* **134,** 1563–1571.

Devy L, Blacher S, Grignet-Debrus C, Bajou K, Masson V, Gerard RD, Gils A, Carmeliet G, Carmeliet P, Declerck PJ, Noël A and Foidart J-M. (2002). *FASEB J.,* **16,** 147–154.

Duffy MJ, O'Grady P, Devaney D, O'Siorain L, Fennelly JJ and Lijnen HJ. (1988). *Cancer,* **62,** 531–533.

España F, Estellés A, Fernández PJ, Gilabert J, Sánchez-Cuenca J and Griffin JH. (1993). *Thromb. Haemost.,* **70,** 989–994.

Euhus DM, Hudd C, LaRegina MC and Johnson FE. (1986). *J. Surg. Oncol.,* **31,** 229–234.

Fay WP, Parker AC, Condrey LR and Shapiro AD. (1997). *Blood,* **90,** 204–208.

Feng Q, Liu K, Liu YX, Byrne S and Ockleford CD. (2001). *Placenta,* **22,** 186–199.

Frandsen TL, Holst-Hansen C, Nielsen BS, Christensen IJ, Nyengaard JR, Carmeliet P and Brünner N. (2001). *Cancer Res.,* **61,** 532–537 (erratum appears in Cancer Res, 62, 330, 2002).

Garlanda C, Berthier R, Garin J, Stoppacciaro A, Ruco L, Vittet D, Gulino D, Matteucci C, Mantovani A, Vecchi A and Dejana E. (1997). *Eur. J. Cell Biol.,* **73,** 368–377.

Grøndahl-Hansen J, Christensen IJ, Rosenquist C, Brünner N, Mouridsen HT, Danø K and Blichert-Toft M. (1993). *Cancer Res.,* **53,** 2513–2521.

Grøndahl-Hansen J, Peters HA, van Putten WLJ, Look MP, Pappot H, Rønne E, Danø K, Klijn JGM, Brünner N and Foekens JA. (1995). *Clin. Cancer Res.,* **1,** 1079–1087.

Gundersen HJG, Bendtsen TF, Korbo L, Marcussen N, Møller A, Nielsen K, Nyengaard JR, Pakkenberg B, Sørensen FB, Vesterby A and West MJ. (1988). *APMIS,* **96,** 379–394.

Gutierrez LS, Schulman A, Brito-Robinson T, Noria F, Ploplis VA and Castellino FJ. (2000). *Cancer Res.,* **60,** 5839–5847.

Guy CT, Cardiff RD and Muller WJ. (1992). *Mol. Cell. Biol.,* **12,** 954–961.

Häckel C, Radig K, Röse I and Roessner A. (1995). *Anat. Embryol.,* **192,** 363–368.

Harbeck N, Thomssen C, Berger U, Ulm K, Kates RE, Höfler H, Jänicke F, Graeff H and Schmitt M. (1999). *Breast Cancer Res. Treat.,* **54,** 147–157.

Hewitt R and Danø K. (1996). *Enzyme Protein,* **49,** 163–173.

Hofmann GE, Glatstein I, Schatz F, Heller D and Deligdisch L. (1994). *Am. J. Obstet. Gynecol.,* **170,** 671–676.

Jänicke F, Schmitt M and Graeff H. (1991). *Semin. Thromb. Hemost.,* **17,** 303–312.

Johnsen M, Lund LR, Rømer J, Almholt K and Danø K. (1998). *Curr. Opin. Cell Biol.,* **10,** 667–671.

Kristensen P, Eriksen J and Danø K. (1991). *J. Histochem. Cytochem.,* **39,** 341–349.
Kristensen P, Pyke C, Lund LR, Andreasen PA and Danø K. (1990). *Histochemistry,* **93,** 559–566.
Laird PW, Zijderveld A, Linders K, Rudnicki MA, Jaenisch R and Berns A. (1991). *Nucleic Acids Res.,* **19,** 4293.
Lambert V, Munaut C, Noël A, Frankenne F, Bajou K, Gerard R, Carmeliet P, Defresne MP, Foidart J-M and Rakic J-M. (2001). *FASEB J.,* **15,** 1021–1027.
Lennon G, Auffray C, Polymeropoulos M and Soares MB. (1996). *Genomics,* **33,** 151–152.
Lijnen HR. (2001). *Ann. NY. Acad. Sci.,* **936,** 226–236.
Lin CY, Anders J, Johnson M and Dickson RB. (1999). *J. Biol. Chem.,* **274,** 18237–18242.
Look MP, van Putten WLJ, Duffy MJ, Harbeck N, Christensen IJ, Thomssen C, Kates R, Spyratos F, Fernö M, Eppenberger-Castori S, Sweep CGJF, Ulm K, Peyrat J-P, Martin P-M, Magdelenat H, Brünner N, Duggan C, Lisboa BW, Bendahl P-O, Quillien V, Daver A, Ricolleau G, Meijer-Van Gelder ME, Manders P, Fiets WE, Blankenstein MA, Broët P, Romain S, Daxenbichler G, Windbichler G, Cufer T, Borstnar S, Kueng W, Beex LVAM, Klijn JGM, O'Higgins N, Eppenberger U, Jänicke F, Schmitt M and Foekens JA. (2002). *J. Natl. Cancer Inst.,* **94,** 116–128.
Loskutoff DJ, Curriden SA, Hu G and Deng G. (1999). *APMIS,* **107,** 54–61.
Lund LR, Bjørn SF, Sternlicht MD, Nielsen BS, Solberg H, Usher PA, sterby R, Christensen IJ, Stephens RW, Bugge TH, Danø K and Werb Z. (2000). *Development,* **127,** 4481–4492.
Lund LR, Rømer J, Bugge TH, Nielsen BS, Frandsen TL, Degen JL, Stephens RW and Danø K. (1999). *EMBO J.,* **18,** 4645–4656.
Maglione JE, Moghanaki D, Young LJ, Manner CK, Ellies LG, Joseph SO, Nicholson B, Cardiff RD and MacLeod CL. (2001). *Cancer Res.,* **61,** 8298–8305.
Matrisian LM. (1999). *Curr. Biol.,* **9,** R776–778.
McMahon GA, Petitclerc E, Stefansson S, Smith E, Wong MKK, Westrick RJ, Ginsburg D, Brooks PC and Lawrence DA. (2001). *J. Biol. Chem.,* **276,** 33964–33968.
Montemurro P, Barbuti G, Conese M, Gabriele S, Petio M, Colucci M and Semeraro N. (1999). *Br. J. Haematol.,* **107,** 294–299.
Nekarda H, Schmitt M, Ulm K, Wenninger A, Vogelsang H, Becker K, Roder JD, Fink U and Siewert JR. (1994). *Cancer Res.,* **54,** 2900–2907.
Nielsen BS, Lund LR, Christensen IJ, Johnsen M, Usher PA, Wulf-Andersen L, Frandsen TL, Danø K and Gundersen HJG. (2001a). *Am. J. Pathol.,* **158,** 1997–2003.
Nielsen BS, Sehested M, Duun S, Rank F, Timshel S, Rygaard J, Johnsen M and Danø K. (2001b). *Lab. Invest.,* **81,** 1485–1502.
Nielsen BS, Sehested M, Timshel S, Pyke C and Danø K. (1996). *Lab. Invest.,* **74,** 168–177.
Parfyonova YV, Plekhanova OS and Tkachuk VA. (2002). *Biochemistry (Mosc),* **67,** 119–134.
Pedersen H, Grøndahl-Hansen J, Francis D, Sterlind K, Hansen HH, Danø K and Brünner N. (1994). *Cancer Res.,* **54,** 120–123.
Pepper MS. (2001). *Thromb. Haemost.,* **86,** 346–355.
Pepper MS, Montesano R, Mandriota SJ, Orci L and Vassalli JD. (1996). *Enzyme Protein,* **49,** 138–162.
Prendergast GC, Diamond LE, Dahl D and Cole MD. (1990). *Mol. Cell. Biol.,* **10,** 1265–1269.
Pyke C, Græm N, Ralfkiær E, Rønne E, Høyer-Hansen G, Brünner N and Danø K. (1993). *Cancer Res.,* **53,** 1911–1915.
Pyke C, Kristensen P, Ralfkićr E, Eriksen J and Danø K. (1991). *Cancer Res.,* **51,** 4067–4071.
Riisbro R, Christensen IJ, Piironen T, Greenall M, Larsen B, Stephens RW, Han C, Høyer-Hansen G, Smith K, Brünner N and Harris AL. (2002). *Clin. Cancer Res.,* **8,** 1132–1141.
Rømer J, Bugge TH, Pyke C, Lund LR, Flick MJ, Degen JL and Danø K. (1996). *Nat. Med.,* **2,** 287–292.
Sappino AP, Huarte J, Belin D and Vassalli JD. (1989). *J. Cell Biol.,* **109,** 2471–2479.
Sappino A-P, Huarte J, Vassalli JD and Belin D. (1991). *J. Clin. Invest.,* **87,** 962–970.
Scott RW, Bergman BL, Bajpai A, Hersh RT, Rodriguez H, Jones BN, Barreda C, Watts S and Baker JB. (1985). *J. Biol. Chem.,* **260,** 7029–7034.
Shi HY, Liang R, Templeton NS and Zhang M. (2002). *Mol. Ther.,* **5,** 755–761.
Shulman M, Wilde CD and Köhler G. (1978). *Nature,* **276,** 269–270.
Stamenkovic I. (2000). *Semin. Cancer Biol.,* **10,** 415–433.
Takeuchi T, Harris JL, Huang W, Yan KW, Coughlin SR and Craik CS. (2000). *J. Biol. Chem.,* **275,** 26333–26342.
Tapiovaara H, Alitalo R and Vaheri A. (1996). *Adv. Cancer Res.,* **69,** 101–133.
Tybulewicz VLJ, Crawford CE, Jackson PK, Bronson RT and Mulligan RC. (1991). *Cell,* **65,** 1153–1163.
Werb Z, Ashkenas J, MacAuley A and Wiesen JF. (1996). *Braz. J. Med. Biol. Res.,* **29,** 1087–1097.
Werb Z, Vu TH, Rinkenberger JL and Coussens LM. (1999). *APMIS,* **107,** 11–18.
Wolf C, Rouyer N, Lutz Y, Adida C, Loriot M, Bellocq J-P, Chambon P and Basset P. (1993). *Proc. Natl. Acad. Sci. USA,* **90,** 1843–1847.